Polarized emission characteristics of UV-LED with subwavelength grating

Yuusuke Takashima[1*], Ryo Shimizu[1], Masanobu Haraguchi[1, 2], and Yoshiki Naoi[1, 2]

[1]Graduate School of Advanced Technology and Science, The University of Tokushima, Tokushima 770-8506, Japan
[2]Institute of Technology and Science, The University of Tokushima, Tokushima 770-8506, Japan
[*]E-mail: takashima@ee.tokushima-u.ac.jp

We investigated polarized emission from a GaN-based ultraviolet light-emitting diode (UV-LED) with a subwavelength grating (SWG) on the surface. The electroluminescence (EL) spectra showed that the UV-LED exhibits high polarization selectivity, as high as s-polarization: p-polarization = 4:1 at a wavelength of 360 nm. The polarized EL characteristics were discussed by the theoretical consideration of Bloch modes resulting from the spatial periodicity of the refractive index in the SWG region and also by finite difference time domain calculations to explore the electromagnetic field. We succeeded in demonstrating the feasibility of a highly polarized UV-LED grown on c-plane sapphire.

1. Introduction

Highly polarized UV emission devices were expected to develop various applications, such as a photoalignment device for liquid crystals, a high-resolution imaging device, and a highly sensitive sensor.[1,2] A compact polarization control device with high transmittance is required to develop integrated devices for these applications, and various attempts have been made for their realization. [3-8, 11-28]

A polarizing plate, which was composed of glass, plastic, and metallic wire grids,[3-8] is generally used to control device polarization. The area scale of the polarizing plate, which is more than a square centimeter order, is very large for integrated devices. Particularly in the UV region, the transmittances of both the metallic wire grid and the plastic film polarizer are very low owing to the large photon absorption in the metal or polymer. Thus, a suitable polarizer for the UV region is still not reported.

UV-light-emitting diodes (LEDs) are suitable for integration, and nitride-based UV-LEDs have been developed. Conventional nitride-based UV-LEDs were grown on c-plane sapphire and emitted unpolarized light.[9,10] Although the polarized emission characteristics of nonpolar or semipolar GaN-based LEDs were reported, [11-14] the power of emission was low owing to the poor quality of the nonpolar or semipolar film grown by heteroepitaxy using r-plane sapphire, compared with that from a LED grown on c-plane sapphire. Recently, another method used to control the polarization using photonic crystals has also been applied to 470 nm emission from GaN-based LEDs.[15] However, this method is not suitable for device integration, owing to the large size and complex design of the devices.

One of the candidate devices for resolving the issue for integration, high polarization, and high transmittance is the device using a high-contrast dielectric subwavelength

grating (SWG).[16-28] In the SWG, the pitch of the grating is shorter than the incident wavelength. The Bloch-like eigenmodes within the SWG region resulting from the spatial periodicity of the refractive index distribution interact with the incident light.[18-20,22] As a result, the desirable optical characteristics such as broadband high reflectivity[18-21,24,25,27] and polarization selectivity[16,17,23,26,28] are obtained with optimized structures. This method is preferable for fabricating integrated devices, because the SWG can be fabricated on conventional LED devices with a lithography technique. Also, the high transmittance in those devices is maintained owing to the absence of metal or polymer absorption in the UV region. Thus, the SWG is suitable for the realization of polarized UV emission.

In this paper, we report the optical characteristics of a nitride-based UV-LED with an SWG, grown on c-sapphire in order to investigate the effect of an SWG on the polarization property of the UV-LED. The electromagnetic distributions within the SWG were examined in order to interpret the interaction between the incident light and the Bloch eigenmodes by the finite difference time domain (FDTD) method. The optimized structure was fabricated on top of the UV-LED by electron beam lithography and inductively coupled plasma (ICP) etching. Electroluminescence (EL) spectra of the UV-LED with the SWG were measured, and the SWG optical characteristics were discussed.

2. Experimental procedure

A UV-LED was fabricated on a c-plane sapphire substrate by a metal organic chemical vapor deposition technique. The UV-LED had a 100-nm-thick p-GaN layer, a p-AlGaN layer, AlInGaN/AlGaN multiquantum wells, and n-AlGaN and n-GaN layers on an undoped GaN layer. The emission spectral peak was observed near the wavelength of 365 nm.

The SWG was fabricated by electron beam lithography and ICP etching as follows. First, a resist (ZEP-520A) was diluted with anisole to 1:1, and the resist film with a thickness of about 100nm was spin-coated onto the sample surface at 3000 rpm for 90 s. Secondly, the grating pattern, which has a 200 nm pitch and a grating bar width of 140 nm, was drawn on top of the UV-LED using electron beams with an acceleration voltage of 50 keV, and the pattern was developed by ZED-50N at 293 K for 15 s. After that, a 50 nm Ni film used as the mask for ICP etching was evaporated, and the resist was removed. In the ICP etching, $SiCl_4$, Cl_2, and Ar gases were used. The Ni film was removed by using HF aqua after the ICP process. Finally, a Au/Ni p-contact film with a thickness of 20 nm was evaporated as an electrode, and the sample was annealed to activate a p-type GaN layer. Figure 1 shows the UV-LED structure with the SWG. The grating area size was 1×1 mm^2. The bird's-eye view of the cross section of the SWG fabricated on top of the UV-LED is shown in Fig. 2. The grating pitch and thickness were 200 and 150 nm, respectively, and the SWG was trapezoidal. The EL spectra at a forward current of 20 mA were measured for transverse electric polarization (s-polarization), in which the electric field is parallel to grating fingers, or transverse magnetic polarization (p-polarization), in which the electric field is perpendicular to grating fingers.

3. Results and discussion

We show EL spectra from conventional UV-LEDs in Figs. 3(a) and 3(b). In Fig. 3, open circles indicate the intensity of s-polarization emission, and filled circles indicate that of p-polarization. For the spectra from the UV-LED without the SWG shown in Fig. 3(a), a nearly unpolarized emission is observed in the wavelength region from 360 to 400 nm. On the other hand, the spectra from the UV-LED with the SWG show a polarized emission as indicated in Fig. 3(b). In particular, the polarization ratio, which is defined by s-polarization intensity/ p-polarization intensity, is 4 at the wavelength of 360 nm.

We discuss the optical characteristics of the SWG by using the dispersion relation and electromagnetic field distribution in the SWG. The dispersion relation in the SWG was investigated in order to interpret the physical light behavior in the SWG. The dispersion analysis model was developed on the basis of Karagodsky's theory.[20] We show the schematic model of the SWG for the dispersion analysis in Fig. 4. In this model, the AlGaN-SWG is surrounded by air. We called the model the symmetric model. The refractive indices of AlGaN (n_{AlGaN}) and air (n_{air}) used in this simulation were 2.47+0i and 1+0i for the 360 nm wavelength, respectively.[29] The incident light propagates along the normal direction from the input side to the output side, and the photon energy propagates through only the 0^{th}-order diffraction light.[20] In the SWG region, Bloch waves exist owing to the spatial periodic distribution of refractive index, and the light propagating through the SWG is composed of eigenmodes.[18,20]

In the model, the AlGaN-SWG has a grating thickness (H) of 150 nm and a filling factor (F) of 0.7, which is defined by the grating bar width (w)/grating pitch (Λ) ratio. The wavelength of incidence in air (λ_0) is 360 nm. When we assumed that the nominal

p-polarization incident light propagated from the input side to the output side, three propagating modes, which are of the 1st, 2nd, and 3rd orders, were found in the region from λ_0/Λ=1 to 1.07. In the region from λ_0/Λ=1.07 to 2, two propagating modes, which are of the 1st and 2nd orders, were obtained. The only 1st -order propagating mode existed when the grating pitch became shorter than half of the incident wavelength. Thus, the p-polarization transmittance through the SWG became smaller in the region from λ_0/Λ=1 to 2, when the 1st- and 2nd-order propagating modes were antiphase and the transmitted light was cancelled. The prediction agreed with the experimental results, indicating the polarized emission in the region of λ_0/Λ=1.825 to 2.

We also investigated the electromagnetic field distribution in the SWG using a two-dimensional FDTD method in order to clarify the optical propagation characteristics of the Bloch modes. In FDTD simulation, the symmetric model, which was the same as the dispersion analysis model, was employed. Figure 5 shows the cross-sectional view of the symmetric model for the simulation. We assumed that the SWG bar has infinite length along the y-direction. The periodic boundary condition was applied in the x-direction, and the perfectly matched layer (PML) boundary condition was also applied in the z-direction. The spatial mesh size was 2nm, and the incremental time in the simulation was 0.47fs. The incident light was employed as the plane wave with a wavelength of 360 nm and propagated from the input side to the output side, because we assumed that the incident light was the emission from the active region in the LED. The refractive indices of AlGaN and air were the same as those used in the dispersion analysis. The transmitted light intensity was evaluated in the measurement plane using the Poynting vector along the z-direction through the SWG. Figure 6 shows the transmittance through the SWG as a function of the incident wavelength/grating

pitch ratio (λ_0/Λ). Two dips at λ_0/Λ=1 and 1.7 for the transmittance spectrum were found for the p-polarization incident wave. The latter indicates the lowest transmittance (4%). The transmittance increases in the region from λ_0/Λ=2 to 6 and saturates to a constant value (about 80%). For the s-polarization wave, the dip in transmittance, which shows the lowest value (about 40%), is obtained at λ_0/Λ=1.4. The highest transmittance for the s-polarization wave is found at λ_0/Λ=1 (about 97%). The magnetic field distribution in the symmetric model at λ_0/Λ=1.7 of the p-polarization wave, namely, the very low transmittance condition, is also shown in Fig. 7. In this figure, the intensity of magnetic field is normalized by that of source field intensity. White and black regions indicate high field intensity; thus, the regions represent a saturated field intensity. A Bloch wave is found in the SWG region, and only the 0^{th}-order diffraction light exists on both the input and output sides. The 1^{st}- and 2^{nd}-order modes were previously observed to be antiphase in the SWG output plane and would cancel each other.[18,20,21)] As a result, the magnetic field intensity of the transmitted light was very low. By FDTD simulation, we found that the light behavior differed between the p- and s-polarization waves in the λ/Λ=1 to 2 region. In particular, the ratio of the transmittance of s-polarization to that of p-polarization was 20 at λ/Λ=1.7. Although the actual grating pitch was in the region of the large transmittance difference, the experimental polarization ratio did not agree with simulation results.

In the actual SWG on top of the LED, the effects of high-order diffractions and light absorption on the optical characteristics should be considered. In previous research studies, however, the effects of high-order diffractions and light absorption on the optical characteristics were not examined.[18-21, 23,-25)] Thus, we employed the asymmetric FDTD model, namely, the SWG on the medium, in order to investigate the mode

behavior in the actual SWG. We show the schematic asymmetric models without and with light absorption in the FDTD simulation in Figs. 8(a) and 8(b), respectively. The SWG was placed on AlGaN in the input region, and the other simulation conditions were the same as those of the symmetric model in Fig. 5. The complex refractive index of p-type GaN (n_{GaN}) in Fig. 8(b) was used according to Ref. 30. For example, n_{GaN}= 2.76+0.2435i for 360 nm, 2.46+0.065i for 370 nm, 2.45+0.0571i for 380 nm, and 2.404+0.0166i for 400 nm were used. The output-side medium was air in the asymmetric model. The transmittance through the SWG in the asymmetric model without light absorption is shown in Fig. 9 as a function of λ_0/Λ. For the p-polarization wave, the dip of transmittance is found, and the lowest transmittance of 20% is obtained at λ_0/Λ=1.25. As the grating period becomes shorter in the region from λ_0/Λ=2 to 3, the transmittance increases. In particular, the rapid increase is obtained at λ_0/Λ=2. For the s-polarization wave, the dip of transmittance is obtained at λ_0/Λ=1.25. The transmittance increases softly in the region from λ_0/Λ=1.25 to 1.5, and the rapid increase is also found at λ_0/Λ=1.55. The difference between the transmittance of the s-polarization wave and that of the p-polarization wave is large in the region of λ_0/Λ=1 to 2. The transmitted light intensity ratio (s-polarization/p-polarization) is around 2.

The magnetic field distribution in the asymmetric model without light absorption at λ/Λ=1.8 is also shown in Fig. 10. We found that the modes exist within the SWG and interact with the bulk wave in the input side region. Although only the 0^{th}-order diffraction exists on the output side of the SWG, higher order diffractions exist in the medium (input side). The origin of higher order diffractions is the distraction of the subwavelength condition in the medium because the bulk wavelength is shorter than the

air wavelength. We also found that Bloch waves interact with higher order diffractions in the SWG region.

In addition, we investigated the effects of light absorption due to the poor crystal quality of p-type GaN on the SWG optical characteristics employing the imaginary part refractive index in the asymmetric model. The transmittance in the asymmetric model with light absorption was about half of that without light absorption, and the tendency of transmittance at λ_0/Λ was the same as that without light absorption. We showed the dependence of the SWG polarization characteristic on the incident light wavelength in Fig. 11. The crosses indicate experimental values of the polarization ratio. The open and filled circles indicate simulation values of the polarization ratio without and with light absorption, respectively. The experimental results indicate high polarization ratios of 3 to 4 in the incident light wavelength range from 360 to 370 nm. In the wavelength ranges from 370 to 380 nm and from 380 to 400 nm, the polarization ratio ranges from 2 to 3 and from 1.7 to 2, respectively.

The simulation result without light absorption in p-type GaN shows that the polarization ratio is 2.5 at 360 nm and linearly decreases in the region of the incident light with the wavelength ranging from 360 to 400 nm. On the other hand, the polarization ratio is around 4 in the simulation result with light absorption in p-type GaN for a wavelength of 360 nm. With light absorption, the polarization ratio rapidly decreases in the wavelength region from 360 to 370 nm. For light wavelengths longer than 370 nm, the polarization ratio is around 2.

Compared with the results of simulations with and without light absorption, there was a small difference in the region from 375 to 400 nm. For light wavelengths shorter than 370 nm, the large difference in polarization characteristic between the results of

simulations with and without light absorption was obtained. In the wavelength range from 370 to 400 nm, the simulation result without light absorption agreed with the experimental result, while the large difference in polarization characteristic occurred for wavelengths shorter than 370nm. On the other hand, the result calculated with light absorption coincided with that of the experiment in the wavelength range from 360 to 400 nm. The agreement between the result of the simulation with light absorption and that of the experiment can be explained by considering the effect of complex refractive index p-GaN on the resonance condition. The electric field of p-polarization was along the grating periodicity direction, while that of s-polarization was perpendicular to the grating periodicity direction. Thus, only the p-polarization eigenmodes were affected by the complex refractive index of the grating bar, and the resonance condition for p-polarization differed from that in the case without light absorption.

As a result of FDTD simulation in the asymmetric model with light absorption, we found that the higher order diffractions and light absorption affect the optical characteristics of the SWG. Moreover, we found a large polarization ratio in the FDTD symmetric model as shown in Fig. 5. Thus, it is possible to realize the achievement of highly polarized emission by the repression of higher order diffraction due to the low-index material under the SWG.

4. Conclusions

We demonstrated that a highly polarized emission can be realized from a conventional UV-LED with an SWG structure, and that a polarization ratio (s-polarization/p-polarization) as high as 4:1 can be obtained in the UV region of around 360 nm. We also investigated the effects of higher order diffractions and light absorption on SWG optical characteristics. We found that the SWG optical characteristics, as theoretically, expected, are suitable for the control of UV photonic devices.

Acknowledgments

We would like to thank Prof. S. Sakai of the University of Tokushima for the preparation of UV-LED samples. We would also like to thank Dr. Jin Pin Ao of the University of Tokushima for technical support in the ICP process and Dr. T. Tomita of the University of Tokushima for discussion of the measurement results. This work is in part supported by a Grant-in-Aid for Scientific Research (24560377) from the Japan Society for the Promotion of Science.

References

1) D. H. Choi and Y. K. Cha, Polym. Bull. **48**, 373 (2002).

2) S. Han, W. Jin, D. Zhang, T. Tang, C. Li, X. Liu, Z. Liu, B. Lei, and C. Zhou, Chem. Phys. Lett. **389**, 176 (2004).

3) Z. Y. Yang and Y. F. Lu, Opt. Express **15**, 9510 (2007).

4) J. H. Lee, Y. W. Song, J. G. Lee, J. Ha, K. H. Hwang, and D. S. Zang, Opt. Express **16**, 16867 (2008).

5) G. G. Kang, I. Vartiainen, B. F. Bai, H. Tuovinen, and J. Turunen, Appl. Phys. Lett. **99**, 071103 (2011).

6) Z. Wu, P. E. Powers, A. M. Sarangan, and Q. Zhan, Opt. Lett. **33**, 1653 (2008).

7) J. Ju, Y. A. Han, J. Kim, E. Byeon, S. M. Kim, Y. H. Lee, and C. K. Hwangbo, Jpn. J. Appl. Phys. **52**, 10MA11 (2013).

8) T. Weber, T. Kasebier, A. Szeghalmi, M. Knez, E. B. Kley, and A. Tunnermann, Nanoscale Res. Lett. **6**, 558 (2011).

9) K. Sumiyoshi, M. Tsukihara, K. Kataoka, S. Kawamichi, T. Okimoto, K. Nishino, Y. Naoi, and S. Sakai, Jpn. J. Appl. Phys. **46**, 491 (2007).

10) K. Sumiyoshi, M. Tsukihara, K. Kataoka, S. Kawamichi, T. Okimoto, K. Nishino, Y. Naoi, and S. Sakai, J. Cryst. Growth **298**, 300 (2007).

11) Y. Naoi, K. Ikeda, T. Hama, K. Ono, R. Choi, T. Fukumoto, K. Nishino, S. Sakai, M. S. Lee, and M. Koike, Phys. Status Solidi C **4**, 2810 (2007).

12) N. F. Gardner, J. C. Kim, J. J. Wierer, Y. C. Shen, and M. R. Krames, Appl. Phys. Lett. **86**, 111101 (2005).

13) T. Koyama, T. Onuma, H. Masui, A Chakraborty, B. A. Haskell, S. Keller, U. K. Mishra, J. S. Speck, S. Nakamura, S. P. DenBaars, T. Sota, and S. F. Chichibu, Appl. Phys. Lett. **89**, 091906 (2006).

14) S. You, T. Detchprohm, M. Zhu, W. Hou, E. A. Preble, D. Hanser, T. Paskova, and C. Wetzel, Appl. Phys. Express **3**, 102103 (2010).

15) C. F. Lai, J. Y. Chi, H. H. Yen, H. C. Kuo, C. H. Chao, H. T. Hsueh, J. F. Trevor Wang, C. Y. Huang, and W. Y. Yeh, Appl. Phys. Lett. **92**, 243118 (2008).

16) S. Y. Chou and W. Deng, Appl. Phys. Lett. **67**, 742 (1995).

17) L. Zhuang, S. Schablitsky, R. C. Shi, and S. Y. Chou, J. Vac. Sci. Technol. B **14**, 4055 (1996).

18) C. J. Chang-Hasnain, Semicond. Sci. Technol. **26**, 014043 (2011).

19) Y. Zhou, M. C. Y. Huang, C. Chase, V. Karagodsky, M. Moewe, B. Pesala, F. G. Sedgwick, and C. J. Chang-Hasnain, IEEE J. Sel. Top. Quantum Electron. **15**, 1485 (2009).

20) V. Karagodsky, F. G. Sedgwick, and C. J. Chang-Hasnain, Opt. Express **18**, 16973 (2010).

21) T. T. Wu, Y. C. Syu, S. H. Wu, W. T. Chen, T. C. Lu, S. C. Wang, H. P. Chiang, and D. P. Tsai, Opt. Express **20**, 20551 (2012).

22) V. Karagodsky, B. Pesala, F. G. Sedgwick, and C. J. Chang-Hasnain, Opt. Lett. **35**, 4099 (2010).

23) G. Zhang, C. Wang, B. Cao, Z. Huang, J. Wang, B. Zhang, and K. Xu, Opt. Express **18**, 7019 (2010).

24) Y. Laaroussi, C. Chevallier, F. Genty, N. Fressengeas, L. Cerutti, T. Taliercio, O. Gauthier-Lafaye, P. F. Calmon, B. Reig, J. Jacquet, and G. Almuneau, Opt. Mater. Express **3**, 1576 (2013).

25) C. Chase, Y. Rao, W. Hofmann, and C. J. Chang-Hasnain, Opt. Express **18**, 15461 (2010).

26) L. Zhang, J. H. Teng, S. J. Chua, and E. A. Fitzgerald, Appl. Phys. Lett. **95**, 261110 (2009).

27) H. Li, W. Li, A. Wu, C. Qiu, Z. Sheng, X. Wang, S. Zou, and F. Gan, Opt. Eng. **52**, 068001 (2013).

28) L. Zhang, J. Teng, S. J. Chua, and E. A. Fitzgerald, Appl. Phys. A **103**, 827 (2011).

29) D. Brunner, H. Angerer, E. Bustarret, F. Freudenberg, R. Hopler, R. Dimitrov, O. Ambacher, and M. Stutzmann, J. Appl. Phys. **82**, 5090 (1997).

30) T. Iwanaga, T. Suzuki, S. Yagi, and T. Motooka, J. Appl. Phys. **98**, 104303 (2005).

Figure caption

Fig. 1. Profile of UV-LED structure with the SWG. The SWG was fabricated on top of UV-LED using electron beam and ICP etching technique.

Fig. 2. Cross-sectional view of the SWG fabricated on top of conventional UV-LED. The grating thickness and pitch are 150 and 200 nm, respectively. The grating profile is trapezoidal.

Fig. 3. Emission spectra from UV-LED: (a) without the SWG structure at a forward current of 20 mA. The peak wavelength of the emission spectra is 365 nm. The spectra show an unpolarized emission in the wavelength range from 360 to 400 nm due to the crystal growth along the c-axis and (b) with the SWG structure on top of the surface at a forward current of 20 mA. The peak wavelength of the emission spectra is 365 nm. The spectra show a polarized emission in the wavelength range from 360 to 400 nm.

Fig. 4. Schematic view of SWG cross section. The SWG input plane is z=0, and the output plane is z=H. The grating bar represents a high-refractive-index material (AlGaN with a refractive index of 2.47+0i for 360 nm) and the surrounding material is air. The nominal incident is polarized with s-polarization and p-polarization.

Fig. 5. Schematic of the symmetric model in FDTD simulation. The wavelength of the plane incident wave is 360 nm, and the wave propagates along the z-direction. The symbols Λ and H indicate the grating period and grating thickness, respectively. The AlGaN-SWG is surrounded by air. The refractive indices of AlGaN and air are respectively 2.47+0i and 1+0i for light with a wavelength of 360 nm. SWG grating length in infinity for y-direction. The PML boundary condition was used for the z-direction, and the periodic boundary condition was also used for the x-direction. The special mesh grid size is 2nm, and the incremental time is 47fs.

Fig. 6. Dependence of the transmittance through the SWG on the grating period and polarization, and F is 0.7. For the p-polarization incidence, the local minimum of 4% is obtained at $\lambda_0/\Lambda=1.7$. For the s-polarization incidence, the minimum value of 40% is obtained. As the grating becomes shorter than half of the incident wavelength, the value of the transmittance becomes constant for both p-polarization and s-polarization.

Fig. 7. Magnetic field distribution within the SWG for p-polarization incidence in FDTD simulation. The magnetic field intensity was normalized by the source field intensity. White and black regions indicate a saturated field intensity. The SWG parameters are H=150 nm, F=0.7, and λ_0/Λ=1.7. Only the 0^{th}-order diffraction exists outside of the SWG, and the higher order diffractions are in the evanescent mode. In the SWG, the interaction between the incidence and the propagating modes was observed.

Fig. 8. Schematic asymmetric model in FDTD simulation. (a) The AlGaN grating was placed on the AlGaN medium. The gap in the SWG is air. The other conditions are the same as those considered in the symmetric model. (b) The AlGaN grating was placed on the AlGaN medium and 100 nm p-type GaN on the AlGaN grating. In p-type GaN, the complex refractive index was used. The other conditions are the same as those considered in the symmetric model.

Fig. 9. Dependence of the SWG transmittance on the grating period and polarization. The filling factor is 0.7. The local minimum is obtained for both polarizations at λ_0/Λ=1.25. The large difference in transmittance between the two polarizations is also found in the region from λ_0/Λ=1 to 2.

Fig. 10. Magnetic distribution of the SWG in the FDTD asymmetric model. The magnetic field intensity was normalized by the source field intensity. White and black regions indicate a saturated field intensity. Athough only the 0^{th}-order diffraction exists in the air region outside of the SWG (output side), higher order diffractions exist in the medium (input side) owing to the light wavelength being shorter than the air wavelength. In the SWG, the modes exist and interact with the higher order bulk wave.

Fig. 11. Dependence of the SWG polarization characteristic on the incident wavelength. In the SWG without light absorption, the result does not agree with the experimental result. In particular, the large difference between the simulation and experimental results is obtained in the incident light wavelength range from 360 to 370nm, although good fit is obtained by considering the light absorption in p-type GaN.

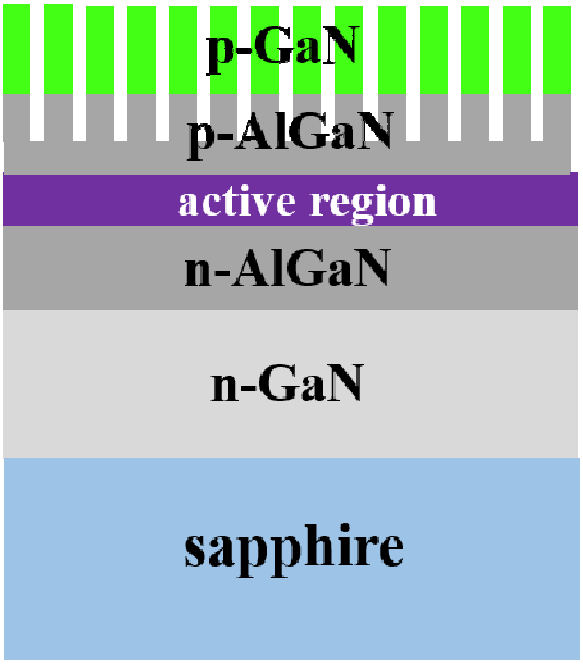

Figure 1

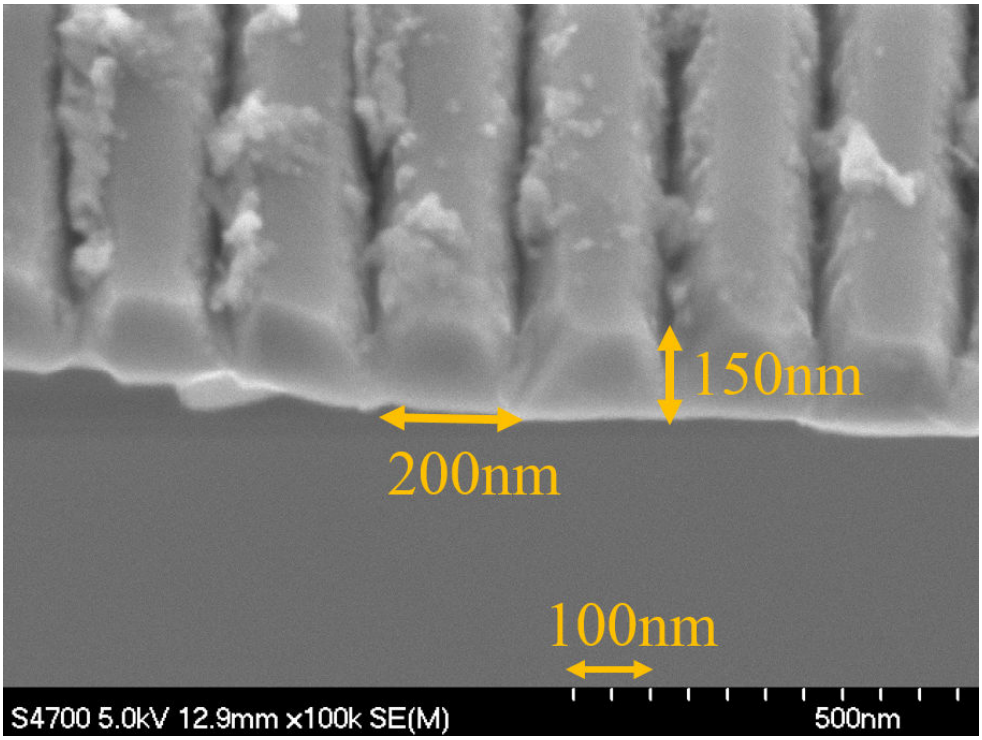

Figure 2

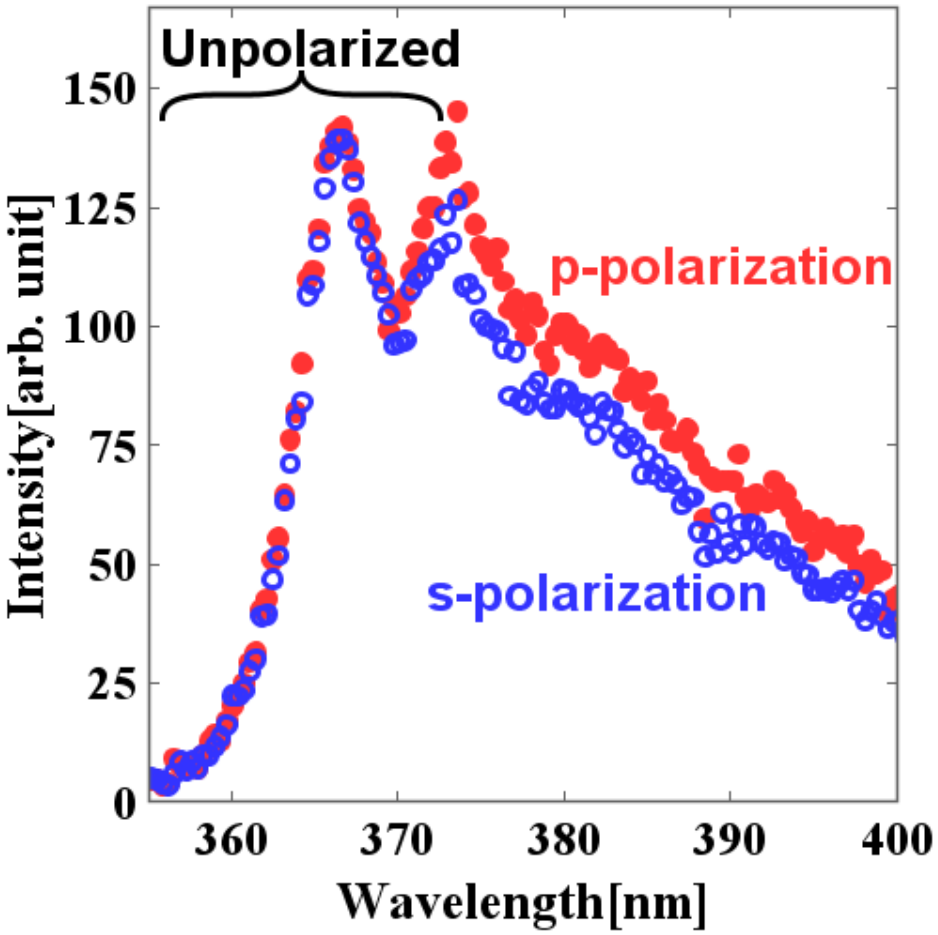
Unpolarized
p-polarization
s-polarization
Intensity[arb. unit]
Wavelength[nm]
0
25
50
75
100
125
150
360
370
380
390
400

Figure 3 (a)

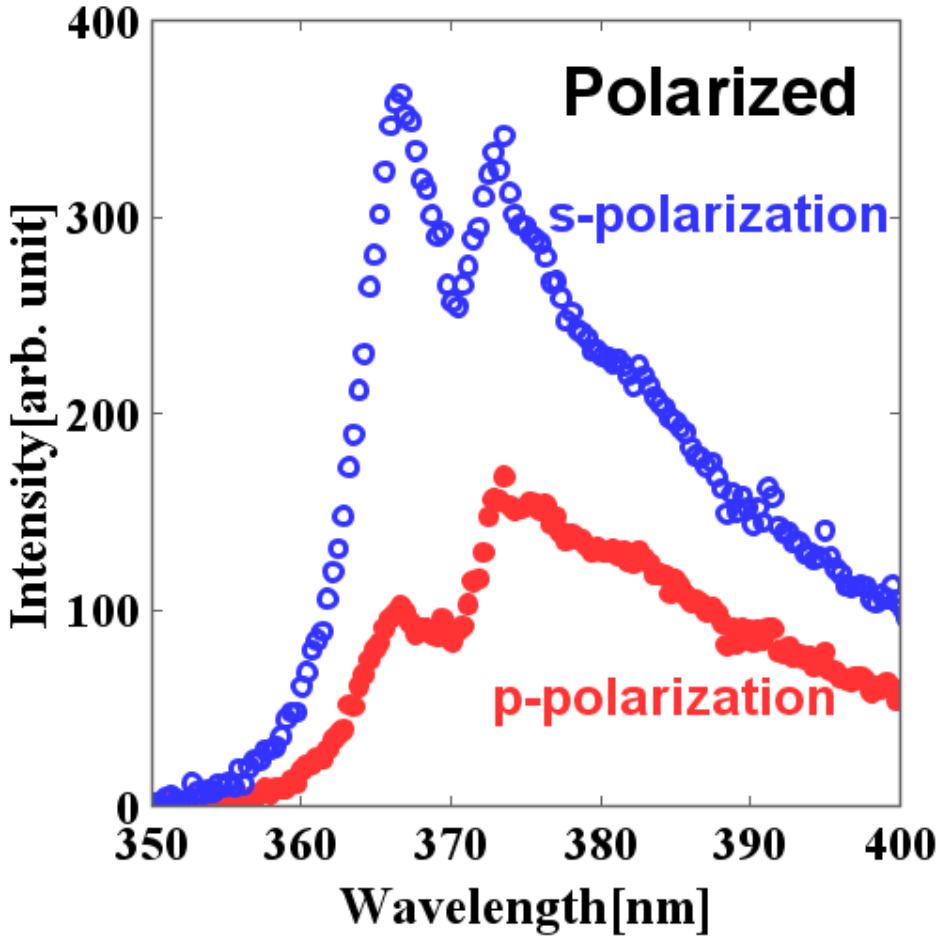
Polarized
s-polarization
p-polarization
Intensity[arb. unit]
Wavelength[nm]
0
100
200
300
400
350
360
370
380
390
400

Figure 3 (b)

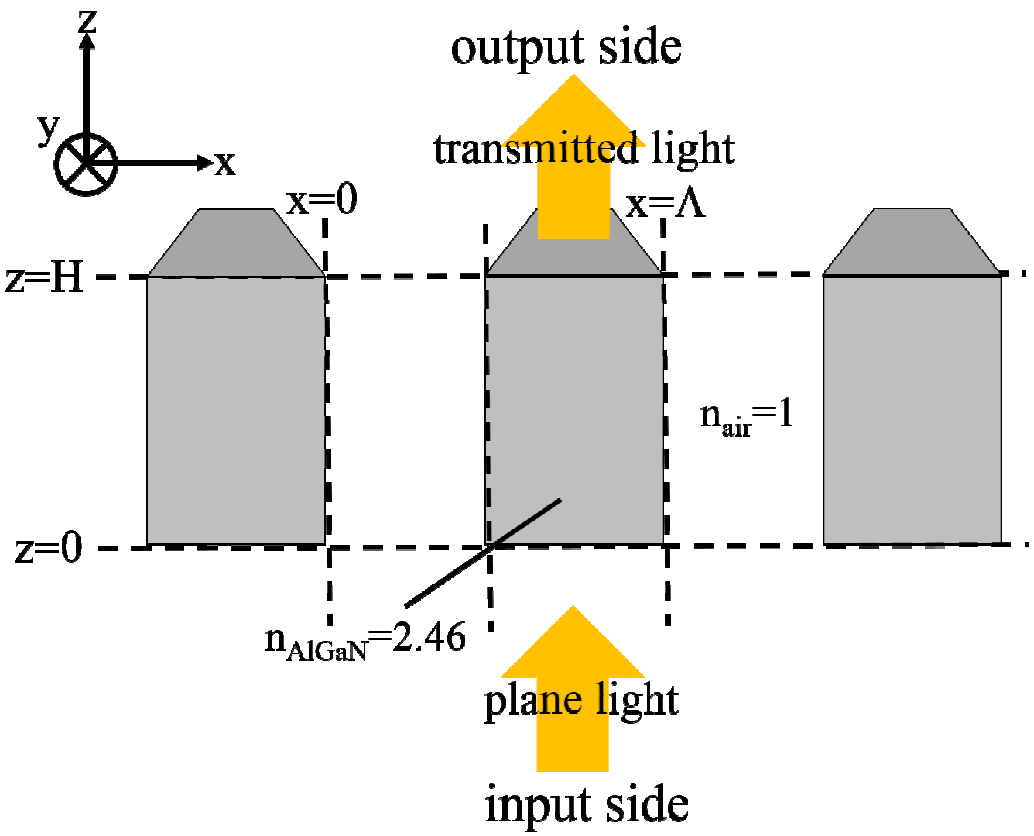
z
y
x
output side
transmitted light
x=0
x=Λ
z=H
n_air=1
z=0
n_AlGaN=2.46
plane light
input side

Figure 4

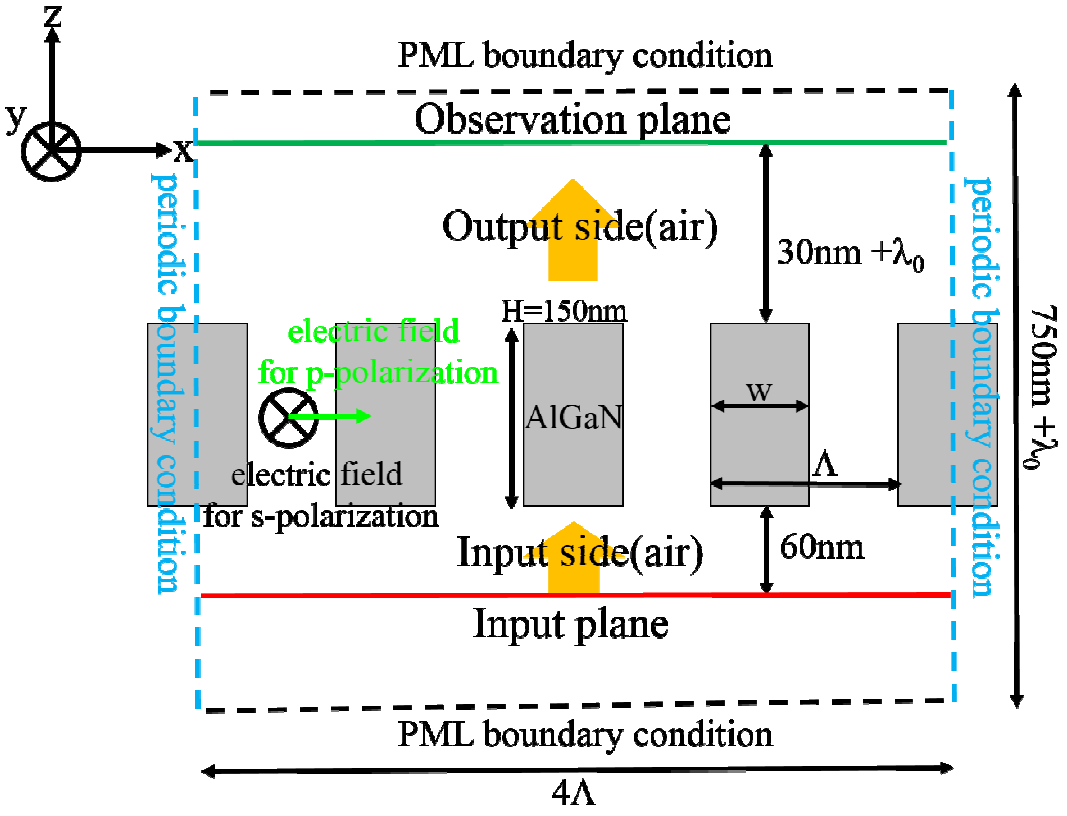
z
y
x
PML boundary condition
Observation plane
Output side(air)
30nm +λ0
periodic boundary condition
periodic boundary condition
750nm +λ0
H=150nm
electric field
for p-polarization
AlGaN
w
Λ
electric field
for s-polarization
Input side(air)
60nm
Input plane
PML boundary condition
4Λ

Figure 5

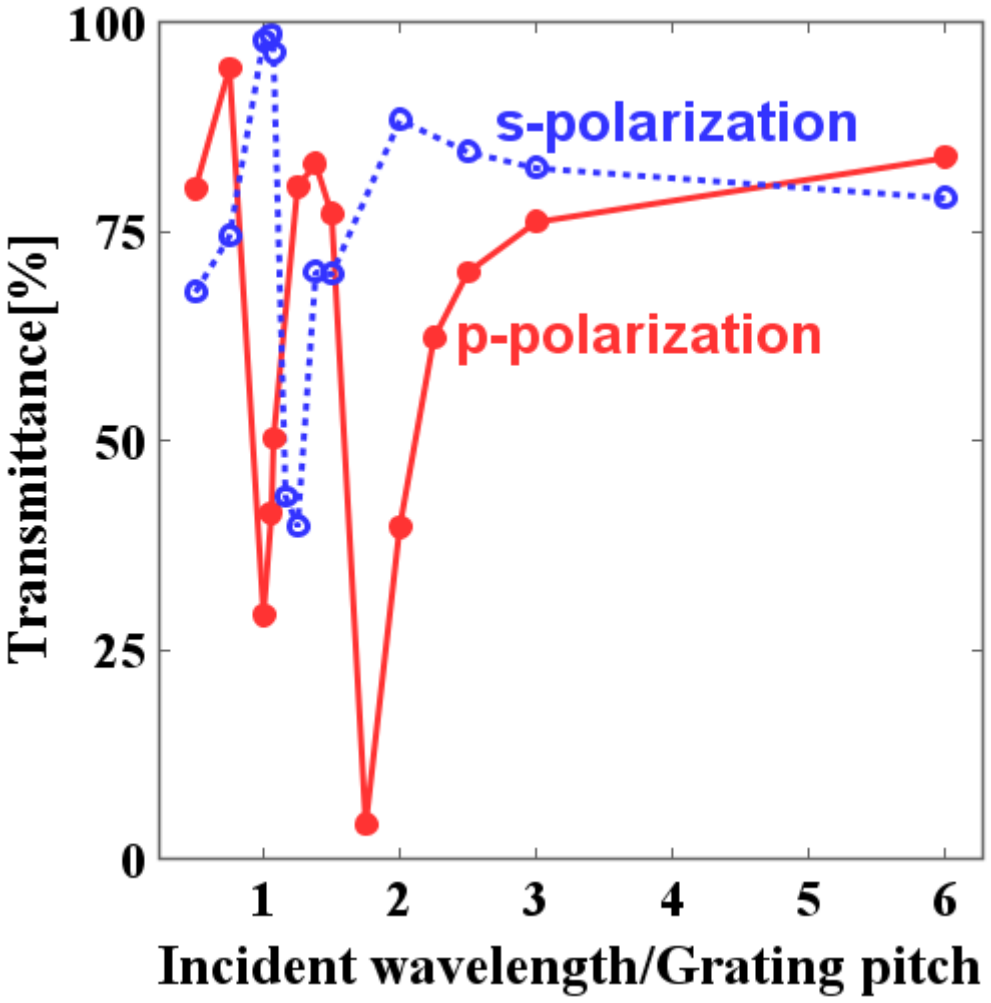
100
75
50
25
0
Transmittance[%]
s-polarization
p-polarization
1
2
3
4
5
6
Incident wavelength/Grating pitch

Figure 6

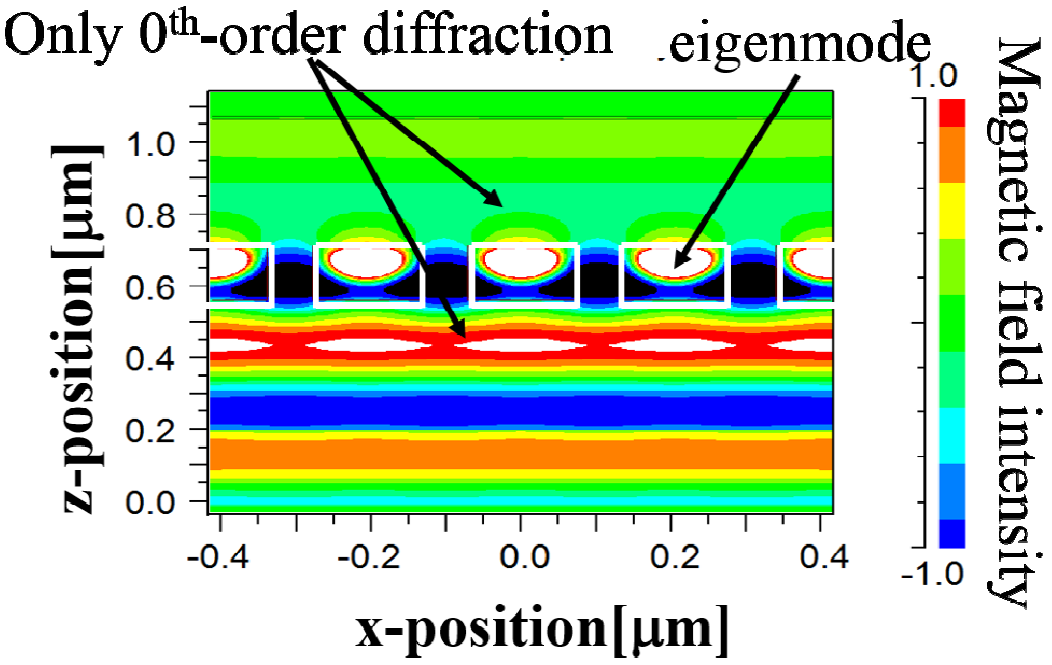
Only 0th-order diffraction
eigenmode
z-position[μm]
1.0
0.8
0.6
0.4
0.2
0.0
-0.4
-0.2
0.0
0.2
0.4
x-position[μm]
1.0
-1.0
Magnetic field intensity

Figure 7

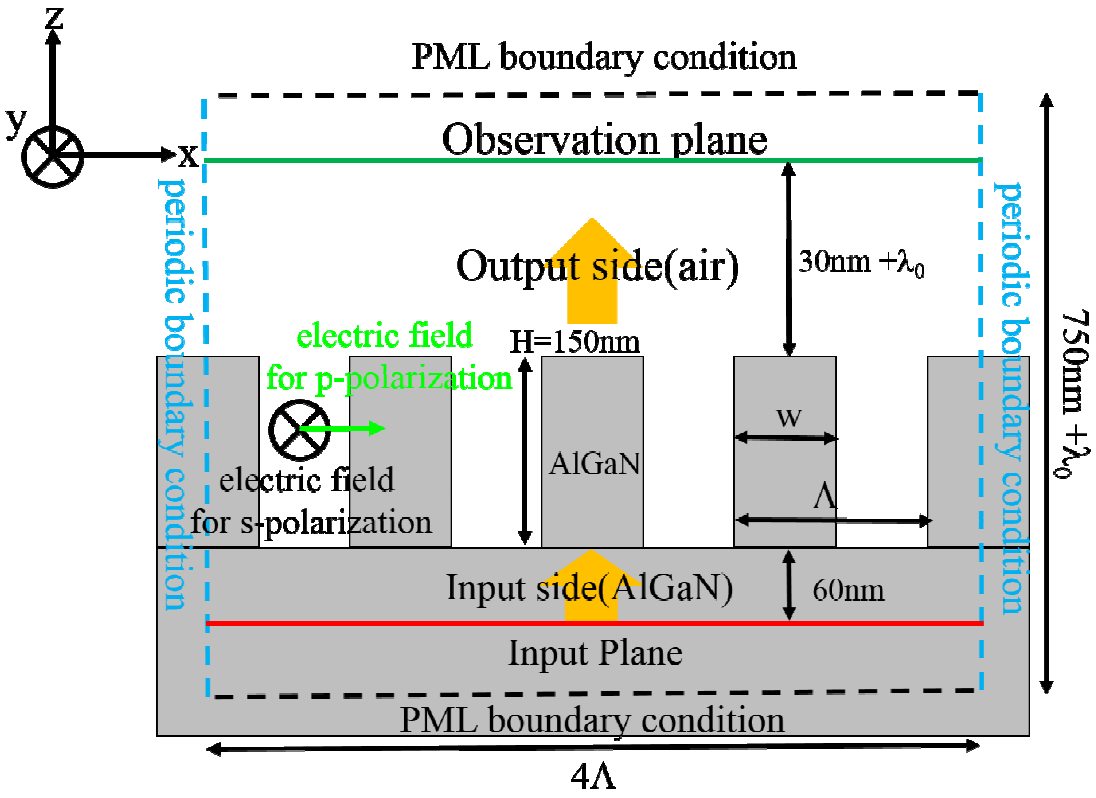
z
y
x
PML boundary condition
Observation plane
periodic boundary condition
Output side(air)
30nm +λ0
electric field
for p-polarization
H=150nm
electric field
for s-polarization
AlGaN
w
Λ
Input side(AlGaN)
60nm
Input Plane
PML boundary condition
periodic boundary condition
750nm +λ0
4Λ

Figure 8(a)

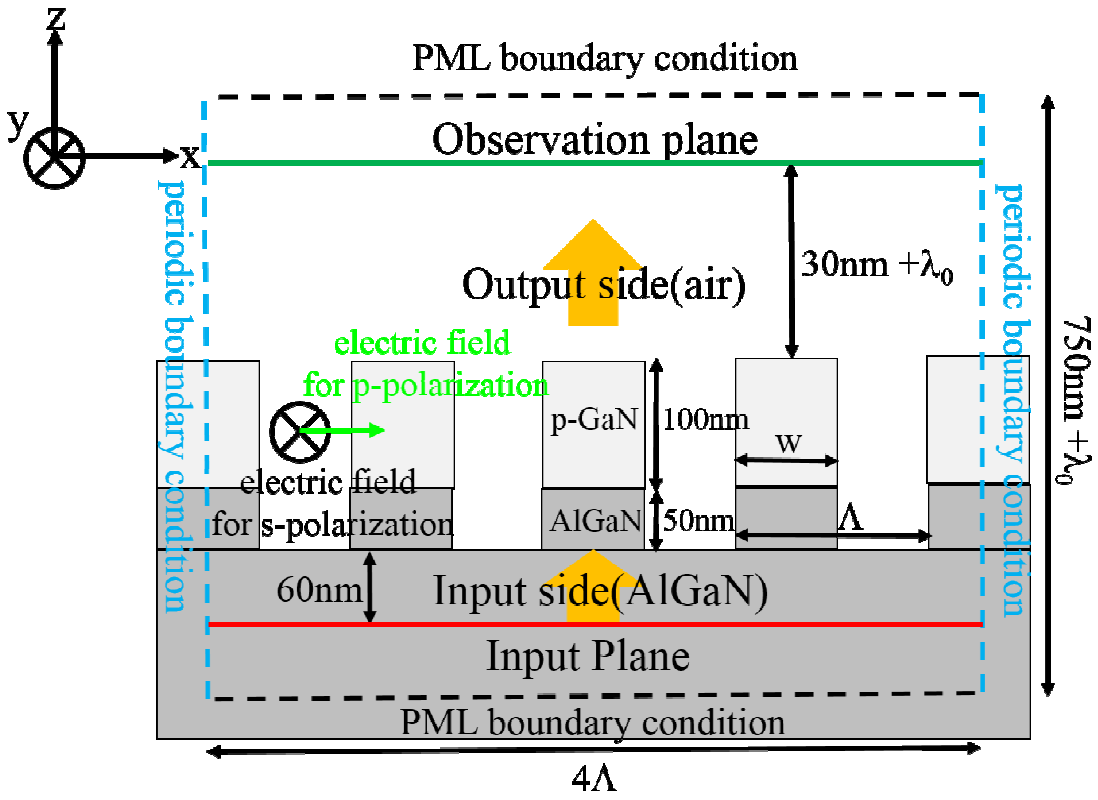
z
y
x
PML boundary condition
Observation plane
periodic boundary condition
periodic boundary condition
Output side(air)
30nm +λ0
750nm +λ0
electric field
for p-polarization
electric field
for s-polarization
p-GaN
100nm
w
AlGaN
50nm
Λ
60nm
Input side(AlGaN)
Input Plane
PML boundary condition
4Λ

Figure 8(b)

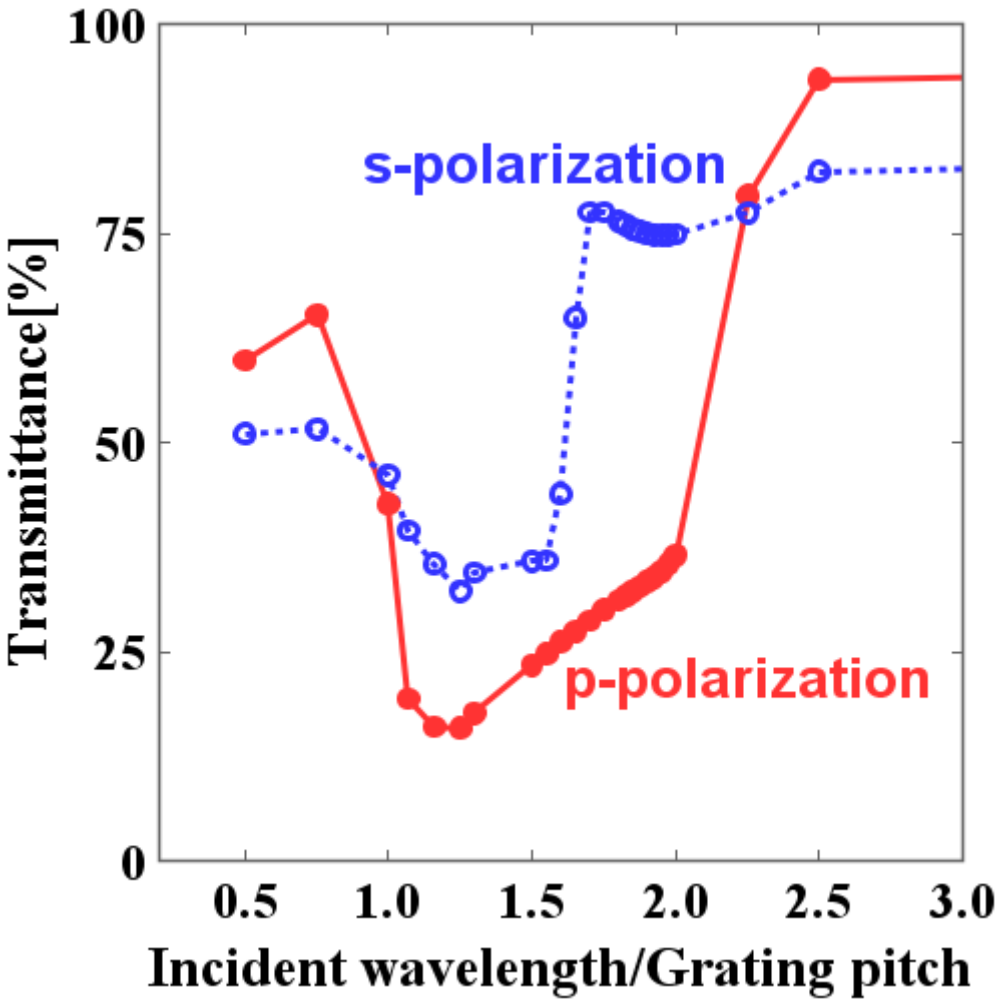
100
75
50
25
0
Transmittance[%]
s-polarization
p-polarization
0.5
1.0
1.5
2.0
2.5
3.0
Incident wavelength/Grating pitch

Figure 9

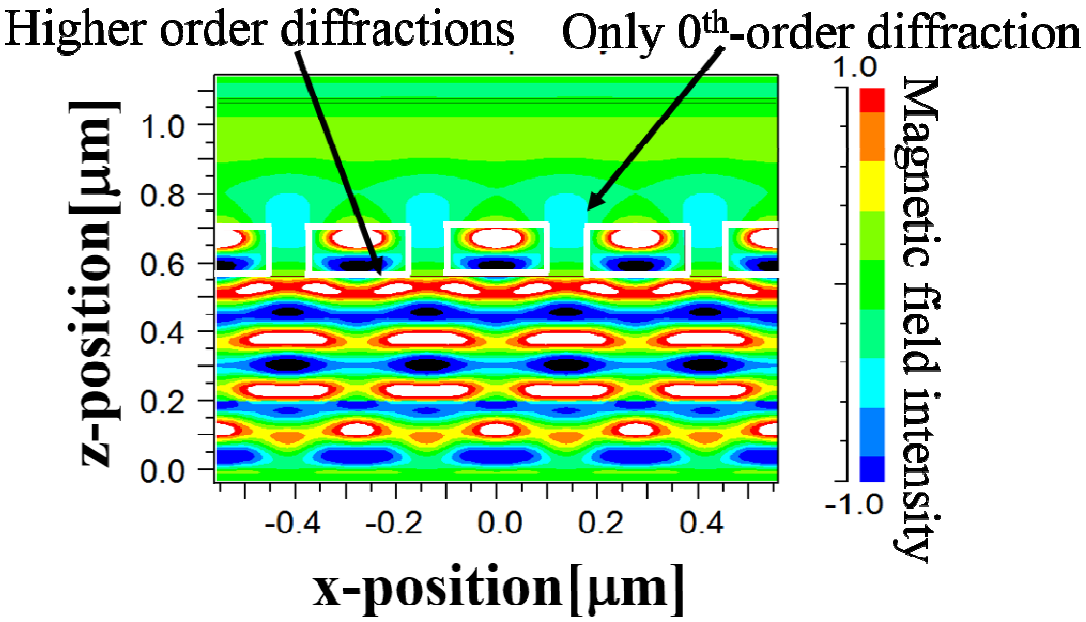
Higher order diffractions
Only 0th-order diffraction
z-position[μm]
1.0
0.8
0.6
0.4
0.2
0.0
-0.4
-0.2
0.0
0.2
0.4
x-position[μm]
1.0
-1.0
Magnetic field intensity

Figure 10

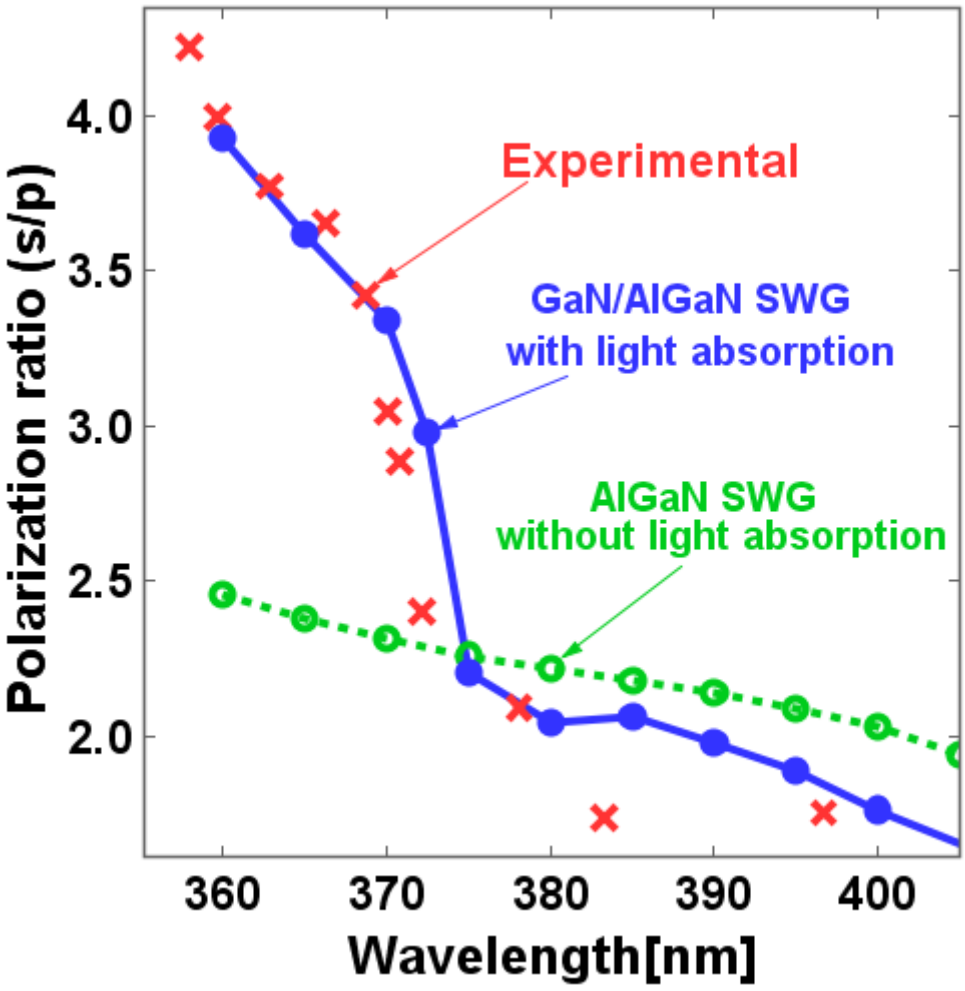
Polarization ratio (s/p)
4.0
3.5
3.0
2.5
2.0
360
370
380
390
400
Wavelength[nm]
Experimental
GaN/AlGaN SWG
with light absorption
AlGaN SWG
without light absorption

Figure 11